

Cytochrome P450 2J2 is required for the natural compound austocystin D to elicit cancer cell toxicity

Yukiko Kojima¹ | Saki Fujieda¹ | Liya Zhou¹ | Masahiro Takikawa¹ | Kouji Kuramochi¹ | Toshiki Furuya¹ | Ayaka Mizumoto² | Noritaka Kagaya³ | Teppei Kawahara⁴ | Kazuo Shin-ya³ | Shingo Dan⁵  | Akihiro Tomida⁵ | Fuyuki Ishikawa²  | Mahito Sadaie^{1,2} 

¹Department of Applied Biological Science, Faculty of Science and Technology, Tokyo University of Science, Noda, Chiba, Japan

²Department of Gene Mechanisms, Graduate School of Biostudies, Kyoto University, Kyoto, Japan

³National Institute of Advanced Industrial Science and Technology (AIST), Tokyo, Japan

⁴Japan Biological Informatics Consortium (JBIC), Tokyo, Japan

⁵Cancer Chemotherapy Center, Japanese Foundation for Cancer Research (JFCR), Tokyo, Japan

Correspondence

Mahito Sadaie, Department of Applied Biological Science, Faculty of Science and Technology, Tokyo University of Science, 2641 Yamazaki, Noda, Chiba 278-8510, Japan.

Email: msadaie@rs.tus.ac.jp

Funding information

JSPS KAKENHI, Grant/Award Number: JP20K07037; AMED, Grant/Award Number: JP20cm0106113; MEXT KAKENHI, Grant/Award Number: JP19H05655

Abstract

Austocystin D is a natural compound that induces cytochrome P450 (CYP) monooxygenase-dependent DNA damage and growth inhibition in certain cancer cell lines. Cancer cells exhibiting higher sensitivity to austocystin D often display elevated *CYP2J2* expression. However, the essentiality and the role of *CYP2J2* for the cytotoxicity of this compound remain unclear. In this study, we demonstrate that *CYP2J2* depletion alleviates austocystin D sensitivity and DNA damage induction, while *CYP2J2* overexpression enhances them. Moreover, the investigation into genes involved in austocystin D cytotoxicity identified *POR* and *PGRMC1*, positive regulators for CYP activity, and *KAT7*, a histone acetyltransferase. Through genetic manipulation and analysis of multiomics data, we elucidated a role for *KAT7* in *CYP2J2* transcriptional regulation. These findings strongly suggest that *CYP2J2* is crucial for austocystin D metabolism and its subsequent cytotoxic effects. The potential use of austocystin D as a therapeutic prodrug is underscored, particularly in cancers where elevated *CYP2J2* expression serves as a biomarker.

KEYWORDS

austocystin D, cytotoxicity, DNA damage, gene expression, knockout screening

Abbreviations: ABCB1, ATP-binding cassette subfamily B member 1; ATAC-seq, assay for transposase-accessible chromatin using sequencing; AUC, area under the curve; CCD, charge-coupled device; ChIP-seq, chromatin immunoprecipitation sequencing; CHK1, checkpoint kinase 1; CRISPR, clustered regularly interspaced short palindromic repeats; CYP, cytochrome P450; EETs, epoxyeicosatrienoic acids; FDR, false discovery rate; gRNA, guide RNA; H3K4me3, histone H3 trimethylated at lysine 4; IF, immunofluorescence; ING4/5, inhibitor of growth family member 4/5; JFCR39, Japanese Foundation for Cancer Research 39; KAT7, lysine acetyltransferase 7; KICH, kidney chromophobe; KIRP, kidney renal papillary cell carcinoma; MDR1, multidrug resistance protein 1; PGRMC1, progesterone receptor membrane component 1; POLR2A, RNA polymerase II subunit A; POR, cytochrome p450 oxidoreductase; RNA-seq, RNA sequencing; RPA32, replication protein A 32; sgRNA, single-guide RNA; SNAI1, snail family transcriptional repressor 1; THYM, thymoma; TSS, transcription start site; γ -H2AX, histone H2AX phosphorylated at serine 139.

This is an open access article under the terms of the [Creative Commons Attribution-NonCommercial](https://creativecommons.org/licenses/by-nc/4.0/) License, which permits use, distribution and reproduction in any medium, provided the original work is properly cited and is not used for commercial purposes.

© 2024 The Author(s). *Cancer Science* published by John Wiley & Sons Australia, Ltd on behalf of Japanese Cancer Association.

1 | INTRODUCTION

Austocystin D is a natural fungal-derived product,¹ initially identified as a cytotoxic compound against human cells overexpressing the multidrug resistance protein 1 (MDR1) multidrug efflux pump.² Austocystin D exhibits bacterial cytotoxicity³ and DNA-damaging activity⁴ in the presence of mammalian liver microsomes—a source of cytochrome P450 (CYP) oxygenases. This suggests that the compound becomes active only after undergoing enzymatic metabolism. Austocystin D is particularly cytotoxic against a subset of cancer cells compared with normal cells.⁴ This selective efficacy is not necessarily linked to drug efflux activity but rather CYP activity.⁴ Austocystin D induces DNA damage and cell growth inhibition.⁴ The compound shares structural similarities with aflatoxin B1, a substance that, when oxygenated by CYP, becomes reactive toward DNA.⁵ Furthermore, dihydro-austocystin D, wherein a single bond substitutes the carbon–carbon double bond in the vinyl ether moiety, loses its cytotoxic activity.⁴ Hence, it is proposed that after austocystin D is oxygenated by cellular CYP, the metabolized form reacts with DNA, leading to DNA damage and subsequent cell growth inhibition.

Comprehensive correlation analyses of chemical sensitivity and gene expression in hundreds of human cancer cell types have revealed a positive correlation between austocystin D sensitivity and *CYP2J2* expression,^{6,7} with *CYP2J2* being exclusive among the 53 CYP genes analyzed. The cytotoxicity of austocystin D can be alleviated via ketoconazole or compound C11 treatment—CYP inhibitors.^{4,7–9} These inhibitors target specific CYPs that might be involved in oxygenating austocystin D. Importantly, while *CYP2J2* is affected by these inhibitors, other CYP molecules, such as *CYP3A4*, demonstrate more effective inhibition than *CYP2J2*.^{9–12} Therefore, while the potential involvement of *CYP2J2* in the metabolic activation and cytotoxicity of austocystin D has been demonstrated, it remains unresolved whether *CYP2J2* contributes to these activities.

CYP2J2 participates in drug metabolism and cardiovascular homeostasis by catalyzing the oxygenation of compounds and polyunsaturated fatty acids, respectively.¹³ *CYP2J2* expression is enhanced in the heart, intestine, liver, and other tissues.¹⁴ While CYPs are generally highly expressed in the liver for drug metabolism, *CYP2J2* constitutes only 1%–2% of the total CYPs in human liver microsomes,¹⁵ implying predominantly extrahepatic functions. Moreover, in the cardiovascular system, *CYP2J2* converts arachidonic acid to epoxyeicosatrienoic acids (EETs), which induce angiogenesis, anti-inflammation, vasodilation, cell proliferation, and survival.^{13,16} Additionally, *CYP2J2* expression is upregulated in cancerous tissues and cells compared with normal tissues and cells.^{16,17} This upregulation is associated with enhanced proliferation, survival, and migration of carcinoma cells.^{18,19} Hence, as forced expression or administration of EETs promotes these signatures, *CYP2J2* and its oxygenase activity might be exploited in cancer pathogenesis.

This study evaluates whether *CYP2J2* is required for austocystin to elicit its toxicity against cancer cells. We have established the contribution of *CYP2J2* to austocystin D cytotoxicity in human cancer cells. Through genetic screening, we identified factors responsible

for austocystin D cytotoxicity and a regulator of *CYP2J2* expression, providing insights into the underlying molecular features in *CYP2J2*-upregulated cancer cells.

2 | MATERIALS AND METHODS

2.1 | Cell culture and gene transfer

HOS, U-2 OS, SaOS-2 (kindly provided by Roger Reddel), SJS-A1, IMR90 (American Type Culture Collection [ATCC]), G-292 (Japanese Collection of Research Bioresources [JCRB]), HS-OS-1, HuO-3N1, HuO9N2, MG-63, NOS-1, and NOS-2 (RIKEN BRC through the National BioResource Project of MEXT, Japan) cells were cultured in Dulbecco's Modified Eagle Medium (DMEM) supplemented with 10% fetal bovine serum (FBS). Retroviral gene transfer was performed as described previously,²⁰ with minor alterations. Plat-A cells were used for viral packaging,²¹ and PEI MAX (Polysciences, 24765-1) was used for transfection. Lentiviral gene transfer was performed as described elsewhere (Addgene, <https://www.addgene.org/protocols/plko/#E>). For every CRISPR-Cas9-based gene silencing experiment, we transduced the genes for Cas9 and guided RNA (gRNA) into the cells, followed by selection using appropriate antibiotics before conducting further experiments without cell cloning.

2.2 | Plasmids

The pMXs(pur)-*CYP2J2* retroviral plasmid was used. *CYP2J2* cDNA (NCBI: CCDS613) was cloned using U-2 OS mRNA. For CRISPR-Cas9-based gene silencing, the following sequences were designed for gRNA targeting against *CYP2J2*: 5'-GCTCGCGGCGATGGGCTCTC-3' (#1), 5'-CTCTCTGGCGGCTGCCCTCT-3' (#2), 5'-GTGCCAGTAGGAGAGTCCG-3' (#3), 5'-CGGGCGGTTCCCAAAGTTT-3' (#4), 5'-CTGACAGCTAAGGAAGT-3' (#5), 5'-TTAAGATATGTTCTCGCAT-3' (#6), POR: 5'-GCCCCCGCTACGGGATGCG-3' (#1), 5'-ACATGCCTCGCATCCCGTAG-3' (#2), PGRMC1: 5'-CCATGAGTATGCGCGGGTCC-3' (#1), 5'-TCCAGTCAAGTATCATCAG-3' (#2), KAT7: 5'-GACAACCTCACATGTGCCG-3' (#1), 5'-AGAGCCAAACGATACTCCGC-3' (#2), and were expressed by lentiCRISPRv2 (Addgene #52961). The sequence 5'-GGGGCCACTAGGGACAGGAT-3' (*AAVS1*) was used as the negative control.

2.3 | Antibodies and compounds

Antibodies used for Western blotting were against RPA32 (35869, Cell Signaling Technology), CHK1 (2360, Cell Signaling Technology), CHK1-S345ph (2348, Cell Signaling Technology), γ -H2AX (9718, Cell Signaling Technology), *CYP2J2* (PA5-106559, Thermo Fisher Scientific), and β -Actin (60008-1-Ig, Proteintech). Austocystin D was prepared as described in Data S1. Ketoconazole was obtained from TCI (K0045).

2.4 | Assays in the JFCR39 system

Growth inhibition assays using JFCR39 cancer cell lines and subsequent data processing were performed as described previously.^{22–24}

2.5 | Cell viability assay

The cells were treated with austocystin D for 3 days at different concentrations. Cell survival was measured using Cell Counting Kit-8 (Dojindo, CK04), and dead cells were stained with trypan blue.

2.6 | Quantitative reverse transcription-PCR

RNA was prepared using the FastGene RNA Premium Kit (Nippon Genetics, FG-81050) or FastGene RNA Basic Kit (Nippon Genetics, FG-80050) and reverse-transcribed to cDNA using ReverTra Ace qPCR RT Master Mix (Toyobo, FSQ-201) or ReverTra Ace qPCR RT Master Mix with a gDNA remover (Toyobo, FSQ-301). Real-time PCR was performed using THUNDERBIRD Next SYBR qPCR Mix (Toyobo, QPS-201) on a CFX Connect Real-Time PCR Detection System (Bio-Rad). Relative expression levels were calculated using *GAPDH* as an internal control. The following primers were used: *GAPDH*-qPCR_FW (5'-GTCTCCTGACTTCAACAGCG-3'), *GAPDH*-qPCR_RV (5'-ACCACCCTGTTGCTGTAGCCAA-3'), *CYP2J2*-qPCR_FW (5'-CCACCAACTCTTTCAGCAACT-3'), *CYP2J2*-qPCR_RV (5'-GGATTGCCTGTGTGCTTTGAC-3'), *POR*-qPCR_FW (5'-ACTCTGCTCTCGTCAACAGCT-3'), *POR*-qPCR_RV (5'-TGGGTGCTTCTTGGACTCC-3'), *PGRMC1*-qPCR_FW (5'-GGCAAGGTGTTGATGTGAC-3'), *PGRMC1*-qPCR_RV (5'-GCATCTCTTCAGCAAAGACC-3'), *KAT7*-qPCR_FW (5'-AGCCAGAGTTCTCAAGATTCCAGT-3'), *KAT7*-qPCR_RV (5'-GCTGCTGACTACGGGTCACT-3').

2.7 | CRISPR-Cas9 knockout screening

CRISPR-Cas9 gRNA screening was performed as described in Data S1.

2.8 | Immunofluorescence (IF) and microscopic analyses

Immunofluorescence was performed as described previously²⁵ using the γ -H2AX (9718, Cell Signaling Technology) primary antibody and anti-rabbit IgG H&L-Alexa Fluor 488 (ab150061, Abcam) secondary antibody. Cells were fixed with 4% paraformaldehyde on coverslips. The DNA was counterstained with Hoechst 33342. Images were acquired with a wide-field fluorescence microscope AxioVert 200 (Zeiss) equipped with a charge-coupled device (CCD) camera (AxioCam HRc, Zeiss). They were processed accordingly with the AxioVision Rel.4.8 software (Zeiss).

2.9 | Statistical analysis

Statistical analyses were conducted using Prism 7 (GraphPad) (statistical significance was set at $p < 0.05$) software, excluding sgRNA hit identification in CRISPR-Cas9 knockout screening.

2.10 | Databases and web tools

Dependency Map (Depmap) (<https://depmap.org/portal/>); Cancer Cell Line Encyclopedia (CCLE) (<https://sites.broadinstitute.org/ccle/>)^{26–28}; Cancer Therapeutics Response Portal (CTRP) (<https://portals.broadinstitute.org/ctrp.v2.1/>)^{7,29,30}; The Human Protein Atlas (<https://www.proteinatlas.org/>)¹⁴; Gene Expression Omnibus (GEO) (<https://www.ncbi.nlm.nih.gov/geo/>)³¹; GEO2R (<https://www.ncbi.nlm.nih.gov/geo/geo2r/>); Encyclopedia of DNA Elements (ENCODE) (<https://www.encodeproject.org/>)^{32,33}; Galaxy (<https://usegalaxy.eu/>)³⁴; Prognoscan (<http://dna00.bio.kyutech.ac.jp/PrognScan/>)³⁵; UCSC Xena (<https://xena.ucsc.edu/>).³⁶

3 | RESULTS

3.1 | Austocystin D sensitivity positively correlates with higher *CYP2J2* expression in osteosarcoma (OS) cell lines

To confirm the positive correlation between austocystin D sensitivity and *CYP2J2* expression level,⁷ we used data from the Japanese Foundation for Cancer Research 39 (JFCR39)—a panel of 39 human cancer cell lines with comprehensive information, including responses to drugs or gene expression profiles.²³ We first determined the GI_{50} (concentration causing 50% growth inhibition) of austocystin D for 39 cell lines by treating them with five doses of the compound and measuring cell growth inhibition (Figure 1A; Figure S1).²⁴ JFCR39 includes transcriptomic data from a cDNA microarray covering 9216 human genes, in which each cell line's relative mRNA expression level is normalized to a combination of the 39 cell lines.²² To identify genes with high expression in austocystin D-sensitive cells, we selected those with a negative correlation between the GI_{50} and gene expression levels (Table S1). The top 50 over-represented gene probes that indicated low Pearson's r values corresponded to 41 genes. Among them, the expression of one CYP gene, *CYP2J2*, was positively correlated with austocystin D sensitivity (Figure 1B; Table S1) and the correlation was stronger than for other CYP genes (Figure 1C), consistent with a previous report.⁷ Since austocystin D was found to be highly cytotoxic against human cells overexpressing MDR1 (ABCB1),² we also examined the correlation between *ABCB1* expression and austocystin D sensitivity using data stored in the depmap portal; however, no correlation was observed (Figure S2A). Meanwhile, a strong correlation between *CYP2J2* expression and austocystin D sensitivity was observed (Figure S2B).

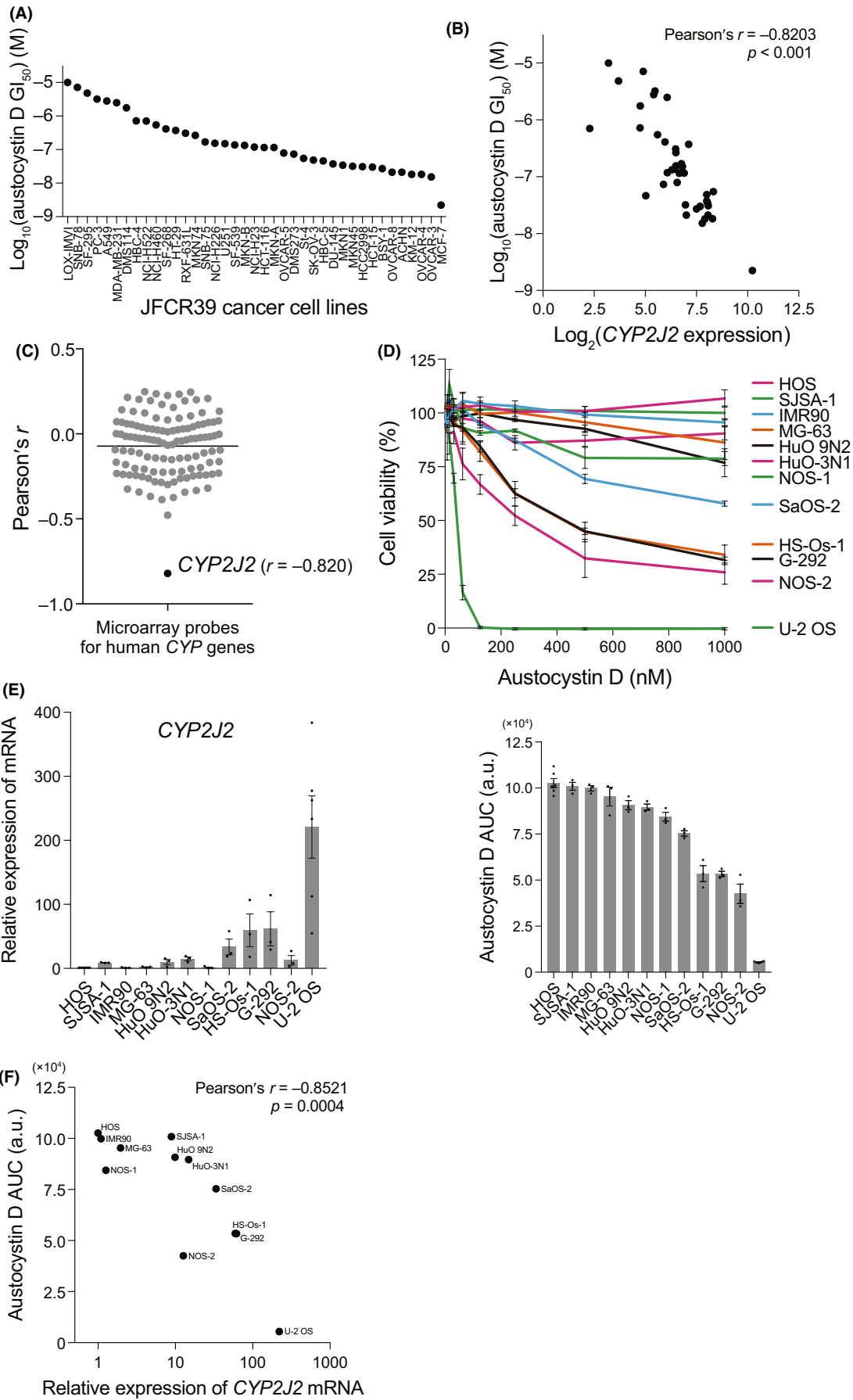


FIGURE 1 Austocystin D sensitivity positively correlates with higher *CYP2J2* expression in JFCR39 and osteosarcoma cell lines. (A) Sensitivity of JFCR39 cell lines to austocystin D is represented by the compound concentration that inhibits 50% of cell growth (GI_{50}). The GI_{50} was determined by treating cells with the compound at 10^{-9} , 10^{-8} , 10^{-7} , 10^{-6} , and 10^{-5} M and measuring cell growth inhibition (Figure S1). (B) *CYP2J2* expression levels and corresponding austocystin D sensitivity in each JFCR39 cell line. Pearson correlation coefficients are shown. (C) Correlation between austocystin D sensitivity in human cells and *CYP2J2* expression is stronger than for other *CYP* genes. Pearson's r values for each microarray probe (66 probes in total) corresponding to 59 human *CYP* genes are shown. The line indicates the mean value. (D) Impact of austocystin D on the viability of 11 human osteosarcoma cell lines and normal fibroblasts (IMR90) at eight concentrations (top panel). The area under the curve (AUC) was calculated using the cell viability curve in (D) (bottom panel). (E) Relative expression of *CYP2J2* mRNA normalized to that in HOS cells measured using quantitative RT-PCR. (F) Correlation analysis between the AUC of (D) and *CYP2J2* expression in (E). Pearson's correlation results are presented. Lines (D) and bars (D, E) represent the mean values for each replicate. Error bars indicate the standard error of the mean.

In some cases, the cells' tissue of origin tends to affect the sensitivity to a compound.³⁷ This tendency may depend on the specific genes expressed in the tissue because cells from the same tissue have similar transcriptional profiles.²² We used data from the depmap portal to assess the tissue specificity of austocystin D sensitivity (Figure S3). The cancer cell lines from the bowel tended to exhibit higher sensitivity. In comparison, those from the central nervous system/brain and lymphoid tissue exhibited lower sensitivity; the underlying transcriptional signature was not investigated. We then examined whether the correlation between austocystin D sensitivity and *CYP2J2* expression was reproducible in 11 human OS cell lines by treating them with serially diluted austocystin D (Figure 1D–F). IMR90 human normal fibroblasts derived from fetal lungs were included in this assay for comparison. The cell lines exhibited different sensitivity levels (Figure 1D). U-2 OS cells exhibited the highest sensitivity, with the smallest area under the curve (AUC). The relative *CYP2J2* mRNA expression level was determined by RT-qPCR, and the ratio of *CYP2J2* to *GAPDH* expression was calculated (Figure 1E). Additionally, our results indicated a correlation between *CYP2J2* expression and austocystin D sensitivity in OS cell lines (Figure 1F). The sensitivity to austocystin D appears to be primarily determined by *CYP2J2* expression, rather than the tissue of origin.

3.2 | DNA damage response and cell death induced by austocystin D treatment

Austocystin D treatment induces different levels of DNA damage, represented by phosphorylation of histone H2AX, among cancer cell lines.⁴ Cells treated with the compound were analyzed by IF using antibodies against the phosphorylated histone H2AX (γ -H2AX) to assess DNA damage. Approximately 20 nM austocystin D treatment increased DNA damage in U-2 OS, not HOS, cells (Figure 2A,B). Immunoblot analysis revealed an increased mobility shift in the RPA32 signal, indicating phosphorylation of RPA32, as well as CHK1 phosphorylation at serine 345 and γ -H2AX under the treatment (Figure 2C). The induction of cell death was also examined via trypan blue staining, indicating that lower concentrations of austocystin D increased the number of dead SaOS-2 and U-2 OS cells compared with HOS cells (Figure 2D). As U-2 OS cells are more sensitive to austocystin D and express a higher level of *CYP2J2* than HOS cells, the

results suggest that cells expressing higher levels of *CYP2J2* cease proliferation by converting austocystin D with *CYP2J2*, followed by DNA damage induction.

3.3 | Overexpression of *CYP2J2* enhances the cytotoxic effects of austocystin D

To investigate whether *CYP2J2* overexpression enhances austocystin D cytotoxicity, we transduced a retroviral vector containing the *CYP2J2* coding sequence into HOS, SaOS-2, and U-2 OS cells (Figure 3A). HOS cells exhibited no loss of viability in the presence of up to 1 μ M austocystin D (Figure 3B, HOS/Vector), whereas U-2 OS and SaOS-2 cells exhibited high and moderate sensitivities, respectively (Figure 3B, U-2 OS/Vector and SaOS-2/Vector). *CYP2J2* overexpression rendered HOS cells highly sensitive to austocystin D and enhanced the sensitivity of SaOS-2 and U-2 OS cells (Figure 3B, HOS/*CYP2J2*, U-2 OS/*CYP2J2* and SaOS-2/*CYP2J2*). In all three cell lines, treatment with 0.5 nM austocystin D in the presence of excess *CYP2J2* increased DNA damage (Figure 3C). Importantly, *CYP2J2* overexpression in the absence of austocystin D had no impact on cell proliferation (Figure S4) or DNA damage (Figure 3C). These results implicate *CYP2J2* in the cytotoxic effects of austocystin D, accompanied by DNA damage induction.

3.4 | Depletion of *CYP2J2* alleviates austocystin D sensitivity

Multi-*CYP* inhibitors, including ketoconazole, can alleviate austocystin D sensitivity in cancer cells.^{4,7} In U-2 OS cells, the observed loss of viability caused by austocystin D treatment was reversed by concurrent treatment with ketoconazole (Figure 4A). Additionally, DNA damage resulting from austocystin D treatment was significantly reduced by ketoconazole treatment (Figure 4B). These results affirm the essential role of *CYP* activity in austocystin D cytotoxicity.

To further investigate the specific contribution of *CYP2J2* to cellular sensitivity to austocystin D, we designed a single-guide RNA (sgRNA) targeting the coding sequences of *CYP2J2*. The genes encoding sgRNA and Cas9 were introduced into cells to suppress

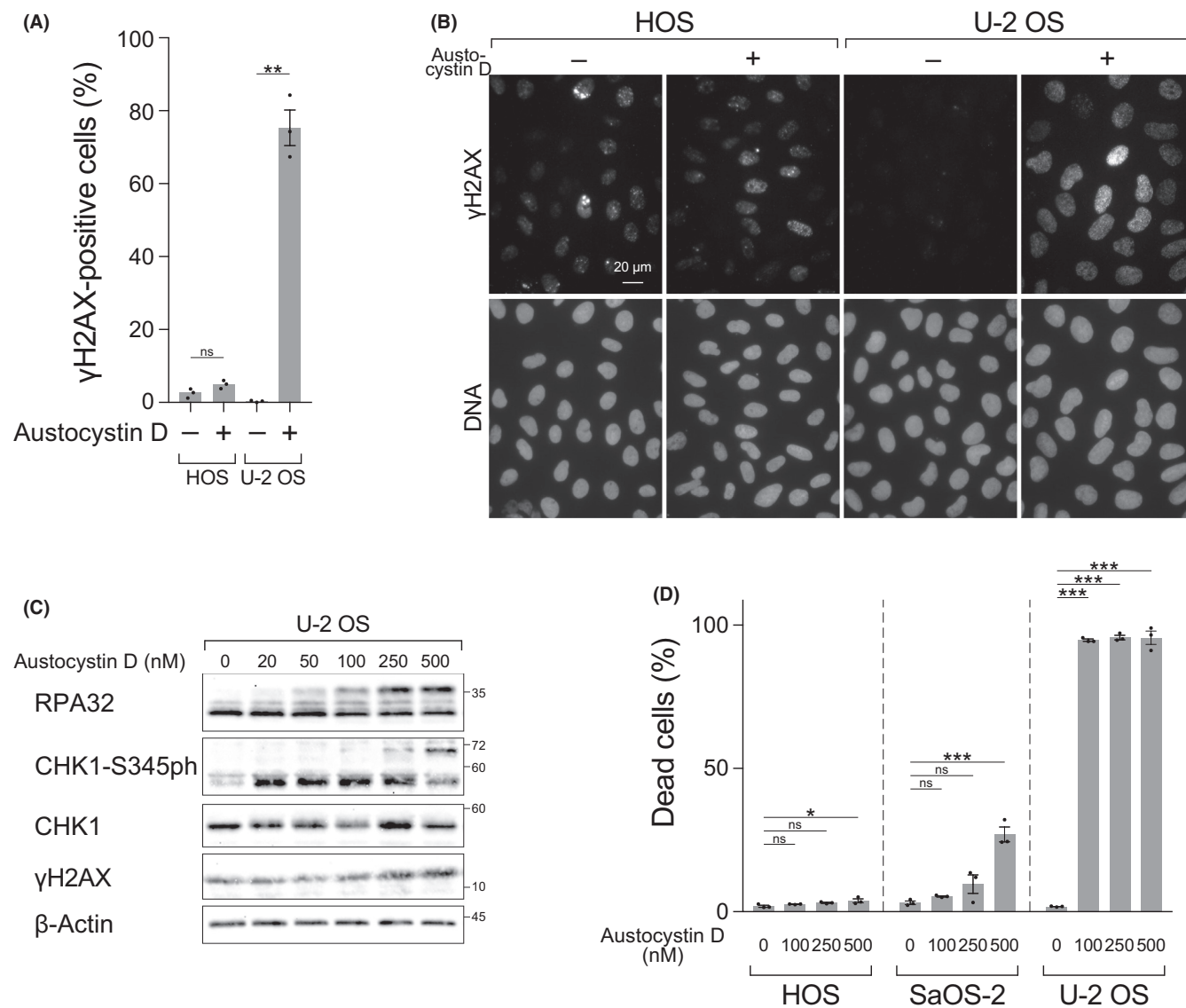


FIGURE 2 The treatment with austocystin D induces DNA damage response and cell death. (A) DNA damage was assessed in U-2 OS cells and HOS cells after treatment with or without 20 nM austocystin D for 24 h. Cells with uniformly stained nuclei, as detected by the anti- γ -H2AX antibody, were considered positive. (B) Representative images of cells treated with austocystin D in (A). Cells were immunostained using anti- γ -H2AX antibodies and counterstained with Hoechst33342. (C) Western blotting with the indicated antibodies for whole-cell extracts from U-2 OS cells treated with austocystin D for 12 h. (D) Dead cells stained with trypan blue after treating cells with austocystin D for 3 days. Bars (A, D) represent the mean values for each replicate. Error bars indicate the standard error of the mean; paired two-tailed t-test (A); one-way analysis of variance (ANOVA) with Dunnett's correction for multiple comparisons (D); *** $p < 0.001$, ** $p < 0.01$, * $p < 0.05$, ns, not significant.

CYP2J2 expression. Three regions were selected as the sgRNA targets. The efficiency of CYP2J2 mRNA suppression in U-2 OS cells was evaluated using RT-qPCR (Figure 4C). Despite attempts to detect intrinsic CYP2J2 protein using various commercial antibodies, no specific signal was obtained (Figure 3A), even in U-2 OS cells, which exhibited the highest level of CYP2J2 mRNA expression among our 11 OS cell lines (Figure 1E). Therefore, the suppression of intrinsic CYP2J2 expression was assessed by RT-qPCR. All types of sgCYP2J2 consistently reduced CYP2J2 mRNA levels (Figure 4C) and mitigated sensitivity to austocystin D (Figure 4D). Due to its superior efficacy in suppressing CYP2J2 expression and austocystin D sensitivity, sgCYP2J2-1 was selected for further analysis. U-2 OS cells

expressing sgCYP2J2 exhibited diminished sensitivity to austocystin D (Figure 4E,F). Moreover, DNA damage induced by austocystin D treatment was significantly reduced in sgCYP2J2-expressing cells (Figure 4G). Hence, CYP2J2 plays a role in the cytotoxic effects of austocystin D.

3.5 | CRISPR-Cas9 gRNA screening identifies genes involved in austocystin D cytotoxicity

Next, we conducted CRISPR-Cas9 gRNA screening to identify gRNA that ameliorates the inhibitory effects of austocystin D

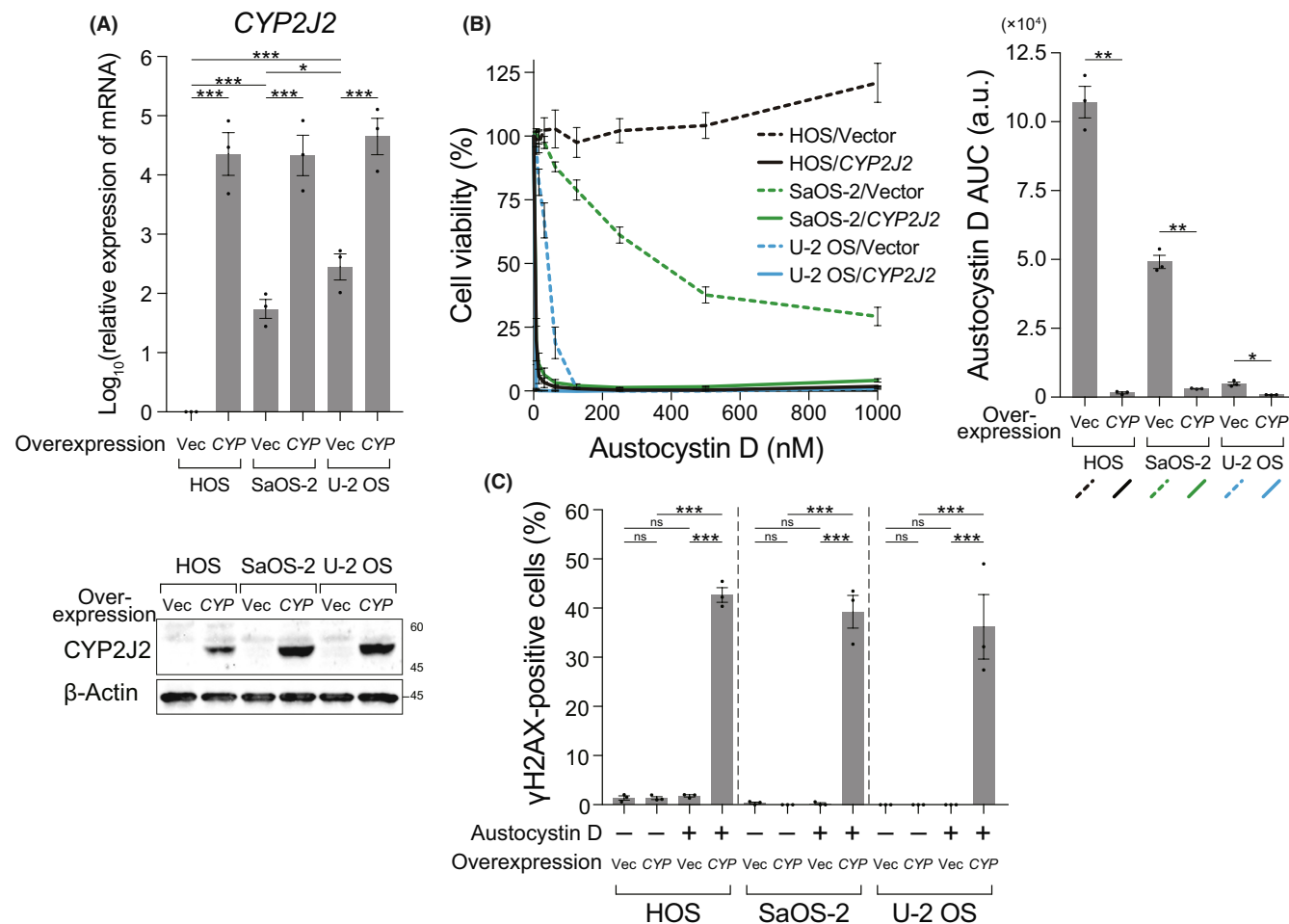


FIGURE 3 Overexpression of CYP2J2 enhances the cytotoxicity and DNA damage induced by austocystin D. (A) Top panel: CYP2J2 expression in cell lines harboring empty or CYP2J2 vectors. The relative expression of CYP2J2 normalized to that in the HOS/Vector cells is presented. Bottom panel: Western blot analysis of protein abundance. (B) Viability of cell lines transduced with the CYP2J2 gene or empty vector treated with various concentrations of austocystin D. AUC was calculated using the cell viability curve in (B). (C) Induction of DNA damage after austocystin D treatment (0.5 nM, 24 h) detected by immunofluorescence using γ -H2AX antibodies. Lines (B) and bars (A–C) represent the mean values for each replicate. Error bars indicate the standard error of the mean; one-way ANOVA with Sidak's correction for multiple comparisons (A, C); paired two-tailed *t*-tests (B); ****p* < 0.001, ***p* < 0.01, **p* < 0.05, ns, not significant.

on proliferation and elucidate factors influencing the CYP2J2-associated regulation of austocystin D cytotoxicity (Figure 5A). The gRNA library was designed with three sgRNAs per gene.³⁸ Pools of U-2 OS cells harboring these sgRNAs were treated or left untreated with austocystin D. Genomic DNA was isolated, and the DNA sequence containing the sgRNA gene was amplified for direct sequencing. Identifying hit genes influencing austocystin D cytotoxicity involved assessing the number of sgRNA genes isolated as hits and the extent of sgRNA gene enrichment after austocystin D treatment (Figure 5B; Table S2).

The sgRNA genes of the top three hit genes (sgPOR, sgPGRMC1, and sgKAT7) that were successfully transduced were enriched in austocystin D-treated cells (Figure 5A), suggesting their involvement in austocystin D cytotoxicity. Although CYP2J2 did not emerge as a significant contributor, one out of three sgRNAs was identified as a hit (Figure 5B, HGLibA_12136). sgCYP2J2-5 (HGLibA_12136) exhibited the most effective mitigation of austocystin D cytotoxicity

(Figure 5C), confirming the screening results (Figure 5B). While the degree of austocystin D sensitivity mitigation by the expression of library-derived sgCYP2J2 was marginal, cells expressing the modified sgRNA—targeting sequences other than those in the sgRNA library—showed apparent resistance to austocystin D compared with cells expressing the negative control sgRNA (Figure 4C,D).

For each of the hit genes (POR, PGRMC1, and KAT7), two sgRNA sequences from the screening were selected, individually introduced into U-2 OS cells, and examined for their impact on austocystin D sensitivity (Figure 5C). Irrespective of the introduced sgRNA, the sensitivity to austocystin D was consistently reduced compared with the control sgRNA, validating the CRISPR-Cas9 gRNA screening results. In the cells expressing each sgRNA, the DNA damage induced by austocystin D treatment was reduced (Figure 5D). Notably, the identification of CYP oxidoreductase (POR)—an electron donor required for CYP-mediated oxidation reactions³⁹—and progesterone receptor membrane component

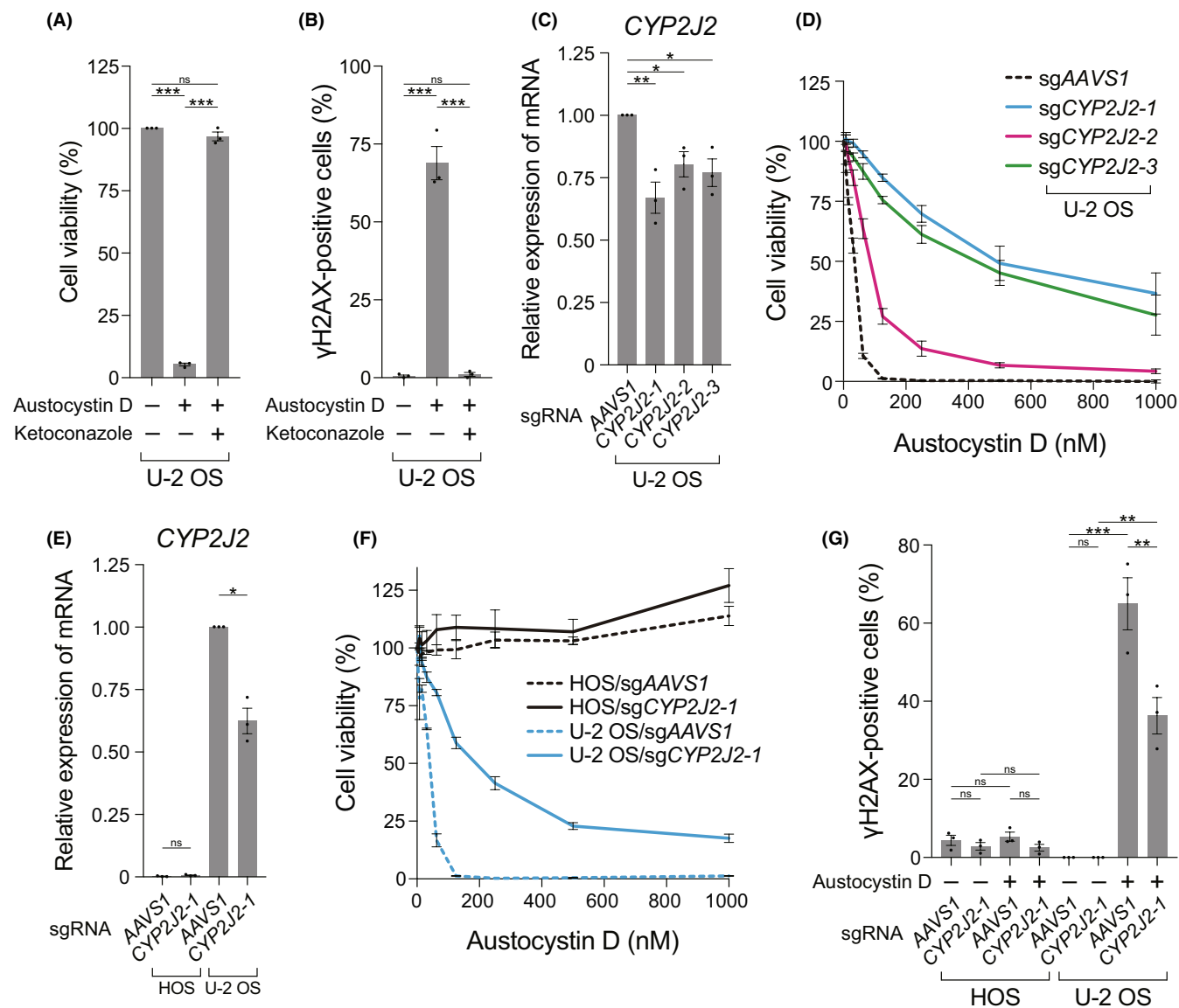
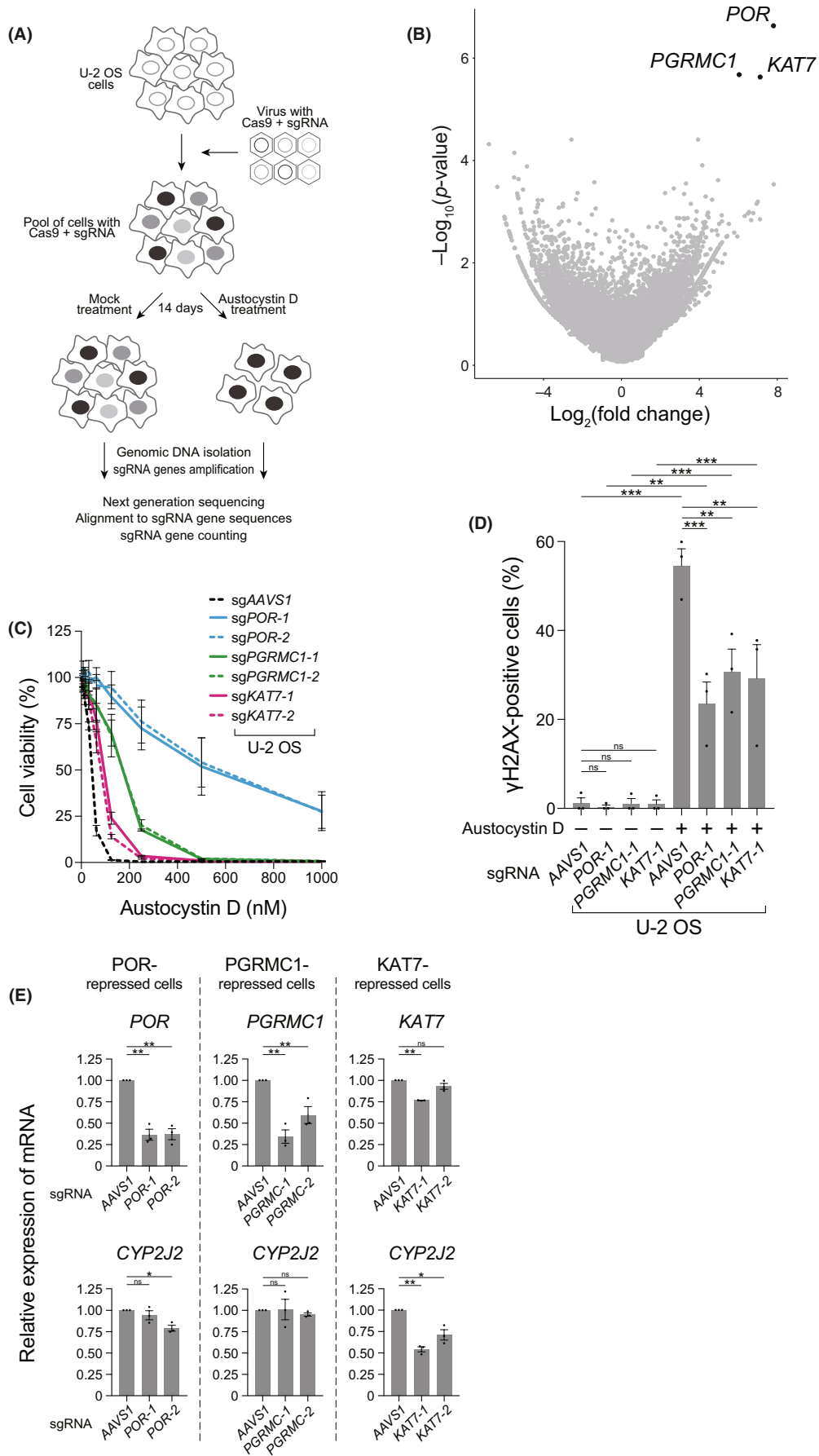


FIGURE 4 Suppression of *CYP2J2* expression reduces austocystin D cytotoxicity. (A) Cell viability after treatment with austocystin D (40 nM, 3 days) with or without 3.75 μ M ketoconazole. (B) DNA damage in U-2 OS cells after treatment with austocystin D (20 nM, 24 h) with or without 3.75 μ M ketoconazole. (C) Relative expression of *CYP2J2* mRNA in U-2 OS cells harboring the Cas9 gene and the single-guide RNA (sgRNA) genes designed against three different *CYP2J2* or *AAVS1* sequences. The relative expression of *CYP2J2* normalized to that in the U-2 OS/sgAAVS1 cells is shown. (D) Cell viability determined after treatment with various concentrations of austocystin D. sgCYP2J2-1 was used for further analyses. (E) *CYP2J2* expression in HOS and U-2 OS cells harboring the Cas9 gene and the sgRNA gene designed against *CYP2J2* or *AAVS1* DNA sequence. The relative expression of *CYP2J2* mRNA is normalized to that in the U-2 OS/sgAAVS1 cells. (F) Cell viability after treatment with various concentrations of austocystin D. (G) DNA damage induced by austocystin D (20 nM, 24 h) in HOS and U-2 OS cells expressing *CYP2J2* sgRNA. Bars (A–C, E, G) and lines (D, F) represent the means for each replicate. Error bars indicate the standard error of the mean; one-way ANOVA with Tukey's correction (A, B), Dunnett's correction (C), and Sidak's correction (G) for multiple comparisons; paired two-tailed *t*-test (E); ****p* < 0.001, ***p* < 0.01, **p* < 0.05, ns, not significant.

FIGURE 5 CRISPR single-guide RNA (sgRNA) screening identifies *POR*, *PGRMC1*, and *KAT7* genes as required for austocystin D cytotoxicity. (A) The sgRNA gene pool was introduced into U-2 OS cells and divided into two groups: One was treated with austocystin D and the other was cultured without treatment. Hit genes were identified as sgRNA target genes upregulated or downregulated in the austocystin D-treated group compared with the untreated group. (B) Volcano plot of significance (negative log *p*-value) versus fold change (log fold change of treated group over untreated group). Genes with a false discovery rate (FDR) < 0.05 are highlighted in black. (C) Cell viability after treatment with various concentrations of austocystin D. U-2 OS cells harboring the Cas9 gene and sgRNA genes targeting the coding sequences of *POR*, *PGRMC1*, *KAT7*, or *AAVS1* were utilized. sgPOR-1, sgPOR-2, sgPGRMC1-1, sgPGRMC1-2, sgKAT7-1, and sgKAT7-2 correspond to HGLibA_37705, 37706, 36288, 36289, 24066, and 24067, respectively, from the sgRNA library. (D) DNA damage induced by austocystin D (20 nM, 24 h) in U-2 OS cells expressing sgRNA targeting the indicated genes. (E) Relative expression of *POR*, *PGRMC1*, *KAT7*, or *CYP2J2* in U-2 OS cells transduced by the indicated sgRNA normalized to that in sgAAVS1-transduced cells. Lines (C) and bars (D, E) indicate the mean values for each replicate. Error bars represent the standard error of the mean; one-way ANOVA with Sidak's correction (D) and Dunnett's correction (E) for multiple comparisons; ****p* < 0.001, ***p* < 0.01, **p* < 0.05, ns, not significant.



1 (PGRMC1), which can bind to and modulate the activity of CYPs,^{40,41} supported the notion that CYP2J2 promotes austocystin D cytotoxicity with the help of POR and PGRMC1. The repression of lysine acetyltransferase 7 (KAT7), which regulates transcription by acetylating histones H3 and H4,^{42,43} led CYP2J2 mRNA downregulation in U-2 OS cells (Figure 5E). Furthermore, reanalysis of microarray data revealed that the expression of CYP2J2 was reduced by KAT7 knockdown⁴⁴ (Figure S6A). The extent of the reduction was most prominent for CYP2J2 compared with other CYP genes (Figure S6B; Table S3). These findings imply that KAT7 promotes CYP2J2 transcription, rendering cells sensitive to austocystin D.

3.6 | KAT7 is enriched at the transcriptionally active CYP2J2 gene

To further investigate KAT7's role in promoting CYP2J2 transcription, we mapped KAT7, RNA polymerase II (POLR2A), histone H3 trimethylated at lysine 4 (H3K4me3), open chromatin, and transcripts on the CYP2J2 locus (Figure S7). We utilized ChIP-seq, ATAC-seq, and RNA-seq data from the ENCODE project. In HepG2 cells, transcripts were mapped on CYP2J2 exons; KAT7, POLR2A, H3K4me3, and ATAC signals were enriched around the transcription start site (TSS; Figure S7, HepG2). Conversely, in K562 cells, where CYP2J2 transcripts were not detected, KAT7 was not enriched at the CYP2J2 locus (Figure S7, K562). Hence, KAT7 directly promotes CYP2J2 transcription, potentially contributing to CYP2J2 upregulation in certain cancer cells.

4 | DISCUSSION

The findings of this study confirm that sensitivity to austocystin D is consistently linked to CYP2J2 expression levels across various cancer cell lines and this correlation is not solely determined by the tissue of origin. CYP2J2 depletion reduces austocystin D sensitivity and mitigates DNA damage induction, while CYP2J2 overexpression exacerbates these phenotypes. Furthermore, through a genome-wide genetic screen, we identified factors that promote CYP enzyme activity and identified a transcriptional activator of CYP2J2. Indeed, the correlation between austocystin D susceptibility and CYP2J2 expression is not coincidental. Rather CYP2J2 is required for austocystin D to elicit its cytotoxic effects (Figure S8).

It has been proposed that CYP enzymes oxygenate the vinyl ether moiety of austocystin D, forming a compound that induces DNA damage and subsequently reduces cell viability.^{3,4} Furthermore, the cytotoxic potential of austocystin D is diminished by CYP inhibitors.^{4,7} Factors promoting CYP activity, POR and PGRMC1, were identified through our genetic screening. Given the various substrates for CYP2J2,¹³ myriad substances can potentially be oxygenated to enhance austocystin D cytotoxicity. Meanwhile, dihydro-austocystin D—a variant in which a single bond replaces the carbon-carbon

double bond in the vinyl ether moiety—essentially loses its cytotoxic activity.⁴ This is attributed to its inability to undergo oxygenation by CYPs. Additionally, the overexpression of CYP2J2 increases austocystin D cytotoxicity and DNA damage. These results strongly suggest that CYP2J2 plays a pivotal role in oxygenating austocystin D, which then induces DNA damage and cytotoxicity. This aligns with the significantly higher correlation of CYP2J2 compared with other CYPs with cellular austocystin D sensitivity.⁷ While other CYPs may be involved in the oxygenation or cytotoxicity of austocystin D, selective perturbation of CYP2J2 expression mitigates the toxic effects and DNA damage induced by austocystin D. To assess the extent of CYP2J2's contribution to the cytotoxicity of austocystin D, it is essential to conduct experiments using knockout cell clones. Our results demonstrate the activation of RPA32 and CHK1, along with H2AX phosphorylation, in the presence of austocystin D. This suggests the accumulation of single-stranded DNA (ssDNA) and the induction of a DNA damage response. Specifically, ATR-mediated phosphorylation of CHK1 and H2AX is involved in this process.^{45–49} Notably, austocystin D induces ssDNA breaks in the presence of CYP activity,⁴ although the underlying mechanism remains unclear. Metabolized forms of austocystin D, produced by CYP2J2, can form bulky adducts on DNA,⁴ resulting in base damage and ssDNA break induction through base excision repair.^{50–52} These adducts may also be repaired by nucleotide excision repair. Additionally, these adducts could lead to replication fork stalling, ultimately resulting in DNA double-strand breaks (DSBs) and subsequent DSB repair. Any scenarios described above could involve RPA binding to ssDNA and the associated DNA damage response.

A previous report proposed that CYP2J2 is predominantly expressed in epithelial cells, increasing their sensitivity to austocystin D.⁷ In that study, *SNAI1* overexpression induced epithelial-to-mesenchymal transition and a consequent reduction in austocystin D sensitivity. However, austocystin D sensitivity and CYP2J2 expression levels vary among OS cell lines derived from mesenchymal cells in the bone,⁵³ suggesting that the cell's tissue of origin does not solely determine sensitivity or expression levels. Based on our observations and a previous report indicating that *SNAI1* overexpression leads to CYP2J2 downregulation,⁵⁴ we propose that the expression level of CYP2J2 and its enzymatic activity, rather than the cells' tissue of origin, determine austocystin D sensitivity. Although the downregulation of *MIRLET7B*—a gene for microRNAs that repress CYP2J2 expression—may upregulate CYP2J2 expression post-transcriptionally,⁵⁵ our data reveal the role of KAT7 in regulating CYP2J2 expression in cancer cells. KAT7 was identified as a candidate gene that promotes austocystin D cytotoxicity; its suppression reduced CYP2J2 expression and alleviated austocystin D cytotoxicity. KAT7 forms a complex with ING4/5 and other proteins, participating in transcriptional regulation by acetylating histones H3 and H4.^{42,43} The KAT7 complex interacts with H3K4me3, a marker of TSS for active genes, via ING4/5.^{56,57} Moreover, by analyzing data from previous work, we observed KAT7 enrichment at the TSS of the actively transcribed CYP2J2 gene. These observations suggest that the protein complex containing the KAT7 acetyltransferase is

recruited to the TSS of *CYP2J2*, promoting its transcription. The regulation of *CYP2J2* mRNA levels, which determine sensitivity to austocystin D, remains unknown. Interestingly, there is no correlation between the mRNA levels of *CYP2J2* and *KAT7* across a panel of cancer cell lines (Figure S9). *KAT7* activity is complex and operates at multiple levels, including expression, binding partners that dictate substrate specificity, and post-translational modification, which can be altered in the context of cancer.⁵⁸

Various strategies can impede the growth of cancer cells overexpressing *CYP2J2*, a catalyst in the promotion of neoplastic traits.^{18,19} These include treatment with the prodrug austocystin D, which is metabolized/activated by *CYP2J2*, and *CYP2J2* inhibitors,^{8,13} although it is crucial to avoid unexpected deleterious effects. The *CYP2J2* inhibitor has the potential to inhibit other CYPs. Moreover, when treating cancers with upregulated *CYP2J2* expression, there is a risk of overdose for cells exhibiting lower expression levels. In contrast, austocystin D is expected to undergo more facile metabolism into a toxic compound in cells with high *CYP2J2* expression. Accordingly, austocystin D may hold more promise than the *CYP2J2* inhibitor. Austocystin D has demonstrated efficacy in suppressing tumor growth in animal models, with enhanced effectiveness when encapsulated in liposomes.⁵⁹ Despite the model showing the distribution of austocystin D in the liver and tumors, the compound is less distributed in the heart—a plausible tissue where *CYP2J2* functions.⁵⁹ Given the marginal effect on normal cells,⁴ austocystin D holds potential as a therapeutic drug for cancers where upregulated *CYP2J2* serves as a biomarker for companion diagnostics. Certain types of cancers, which exhibit worse prognosis with higher *CYP2J2* expression levels (Figure S10),⁶⁰ could be candidates for this treatment.

AUTHOR CONTRIBUTIONS

Yukiko Kojima: Conceptualization; formal analysis; investigation; methodology; visualization; writing – original draft; writing – review and editing. **Saki Fujieda:** Investigation; methodology. **Liya Zhou:** Investigation; methodology. **Masahiro Takikawa:** Methodology; writing – review and editing. **Kouji Kuramochi:** Methodology. **Toshiki Furuya:** Methodology. **Ayaka Mizumoto:** Investigation; methodology. **Noritaka Kagaya:** Investigation; methodology. **Teppei Kawahara:** Investigation; methodology; resources. **Kazuo Shin-ya:** Investigation; methodology; resources; writing – review and editing. **Shingo Dan:** Investigation; methodology; writing – review and editing. **Akihiro Tomida:** Investigation; methodology; writing – review and editing. **Fuyuki Ishikawa:** Conceptualization; funding acquisition; writing – review and editing. **Mahito Sadaie:** Conceptualization; formal analysis; funding acquisition; methodology; supervision; visualization; writing – original draft; writing – review and editing.

ACKNOWLEDGMENTS

We thank Makoto Hayashi (Kyoto University) for providing the materials and Makoto Taniguchi (Genome-Lead) for the technical advice. We thank all members of Ishikawa Laboratory, Shin-ya Laboratory,

Dan Laboratory, Tomida Laboratory, and Sadaie Laboratory for their helpful discussions and support.

FUNDING INFORMATION

This work was supported by P-DIRECT from MEXT and AMED; MEXT KAKENHI (Grant Number JP19H05655) and AMED (Grant Number JP20cm0106113) to F.I.; JSPS KAKENHI (Grant Number JP20K07037) and research support from the Yamada Science Foundation and Kobayashi Foundation to M.S.

CONFLICT OF INTEREST STATEMENT

Fuyuki Ishikawa is an editorial board member of *Cancer Science*. The other authors declare no conflict of interest.

ETHICS STATEMENTS

Approval of the research protocol by an Institutional Reviewer Board: N/A.

Informed Consent: N/A.

Registry and the Registration No. of the study/trial: N/A.

Animal Studies: N/A.

ORCID

Shingo Dan  <https://orcid.org/0000-0002-0022-2725>

Fuyuki Ishikawa  <https://orcid.org/0000-0002-5580-2305>

Mahito Sadaie  <https://orcid.org/0000-0002-3443-5980>

REFERENCES

1. Steyn PS, Vlegaar R. Austocystins. Six novel dihydrofuro (3',2':4,5) furo(3,2-b)xanthenones from *Aspergillus ustus*. *J Chem Soc Perkin 1*. 1974;2250-2256.
2. Ireland C, Aalbersberg W, Andersen R, et al. Anticancer agents from unique natural products sources. *Pharm Biol*. 2008;41:15-38.
3. Kfir R, Johannsen E, Vlegaar R. Mutagenic activity of austocystins—secondary metabolites of *Aspergillus ustus*. *Bull Environ Contam Toxicol*. 1986;37:643-650.
4. Marks KM, Park ES, Arefolov A, et al. The selectivity of austocystin D arises from cell-line-specific drug activation by cytochrome P450 enzymes. *J Nat Prod*. 2011;74:567-573.
5. McLean M, Dutton MF. Cellular interactions and metabolism of aflatoxin: an update. *Pharmacol Ther*. 1995;65:163-192.
6. Krushkal J, Negi S, Yee LM, et al. Molecular genomic features associated with in vitro response of the NCI-60 cancer cell line panel to natural products. *Mol Oncol*. 2021;15:381-406.
7. Rees MG, Seashore-Ludlow B, Cheah JH, et al. Correlating chemical sensitivity and basal gene expression reveals mechanism of action. *Nat Chem Biol*. 2016;12:109-116.
8. Chen C, Li G, Liao W, et al. Selective inhibitors of *CYP2J2* related to terfenadine exhibit strong activity against human cancers in vitro and in vivo. *J Pharmacol Exp Ther*. 2009;329:908-918.
9. Lafite P, Dijols S, Zeldin DC, Dansette PM, Mansuy D. Selective, competitive and mechanism-based inhibitors of human cytochrome P450 2J2. *Arch Biochem Biophys*. 2007;464:155-168.
10. Lee CA, Jones JP 3rd, Katayama J, et al. Identifying a selective substrate and inhibitor pair for the evaluation of *CYP2J2* activity. *Drug Metab Dispos*. 2012;40:943-951.
11. Sai Y, Dai R, Yang TJ, et al. Assessment of specificity of eight chemical inhibitors using cDNA-expressed cytochromes P450. *Xenobiotica*. 2000;30:327-343.

12. Wu Z, Lee D, Joo J, et al. CYP2J2 and CYP2C19 are the major enzymes responsible for metabolism of albendazole and fenbendazole in human liver microsomes and recombinant P450 assay systems. *Antimicrob Agents Chemother*. 2013;57:5448-5456.
13. Sisignano M, Steinhilber D, Parnham MJ, Geisslinger G. Exploring CYP2J2: lipid mediators, inhibitors and therapeutic implications. *Drug Discov Today*. 2020;25:1744-1753.
14. Uhlen M, Fagerberg L, Hallstrom BM, et al. Proteomics. Tissue-based map of the human proteome. *Science*. 2015;347:1260419.
15. Yamazaki H, Okayama A, Imai N, Guengerich FP, Shimizu M. Inter-individual variation of cytochrome P4502J2 expression and catalytic activities in liver microsomes from Japanese and Caucasian populations. *Xenobiotica*. 2006;36:1201-1209.
16. Murray M. CYP2J2 – regulation, function and polymorphism. *Drug Metab Rev*. 2016;48:351-368.
17. Karkhanis A, Hong Y, Chan ECY. Inhibition and inactivation of human CYP2J2: implications in cardiac pathophysiology and opportunities in cancer therapy. *Biochem Pharmacol*. 2017;135:12-21.
18. Jiang JG, Chen CL, Card JW, et al. Cytochrome P450 2J2 promotes the neoplastic phenotype of carcinoma cells and is up-regulated in human tumors. *Cancer Res*. 2005;65:4707-4715.
19. Jiang JG, Ning YG, Chen C, et al. Cytochrome p450 epoxygenase promotes human cancer metastasis. *Cancer Res*. 2007;67:6665-6674.
20. Narita M, Narita M, Krizhanovsky V, et al. A novel role for high-mobility group a proteins in cellular senescence and heterochromatin formation. *Cell*. 2006;126:503-514.
21. Morita S, Kojima T, Kitamura T. Plat-E: an efficient and stable system for transient packaging of retroviruses. *Gene Ther*. 2000;7:1063-1066.
22. Dan S, Tsunoda T, Kitahara O, et al. An integrated database of chemosensitivity to 55 anticancer drugs and gene expression profiles of 39 human cancer cell lines. *Cancer Res*. 2002;62:1139-1147.
23. Kong D, Yamori T. JFCR39, a panel of 39 human cancer cell lines, and its application in the discovery and development of anticancer drugs. *Bioorg Med Chem*. 2012;20:1947-1951.
24. Yamori T, Matsunaga A, Sato S, et al. Potent antitumor activity of MS-247, a novel DNA minor groove binder, evaluated by an in vitro and in vivo human cancer cell line panel. *Cancer Res*. 1999;59:4042-4049.
25. Narita M, Nunez S, Heard E, et al. Rb-mediated heterochromatin formation and silencing of E2F target genes during cellular senescence. *Cell*. 2003;113:703-716.
26. Cancer Cell Line Encyclopedia Consortium; Genomics of Drug Sensitivity in Cancer Consortium. Pharmacogenomic agreement between two cancer cell line data sets. *Nature*. 2015;528:84-87.
27. Ghandi M, Huang FW, Jane-Valbuena J, et al. Next-generation characterization of the cancer cell line encyclopedia. *Nature*. 2019;569:503-508.
28. Barretina J, Caponigro G, Stransky N, et al. The cancer cell line encyclopedia enables predictive modelling of anticancer drug sensitivity. *Nature*. 2012;483:603-607.
29. Basu A, Bodycombe NE, Cheah JH, et al. An interactive resource to identify cancer genetic and lineage dependencies targeted by small molecules. *Cell*. 2013;154:1151-1161.
30. Seashore-Ludlow B, Rees MG, Cheah JH, et al. Harnessing connectivity in a large-scale small-molecule sensitivity dataset. *Cancer Discov*. 2015;5:1210-1223.
31. Edgar R, Domrachev M, Lash AE. Gene expression omnibus: NCBI gene expression and hybridization array data repository. *Nucleic Acids Res*. 2002;30:207-210.
32. The ENCODE Project Consortium. An integrated encyclopedia of DNA elements in the human genome. *Nature*. 2012;489:57-74.
33. Luo Y, Hitz BC, Gabdank I, et al. New developments on the encyclopedia of DNA elements (ENCODE) data portal. *Nucleic Acids Res*. 2020;48:D882-D889.
34. The Galaxy Community. The galaxy platform for accessible, reproducible and collaborative biomedical analyses: 2022 update. *Nucleic Acids Res*. 2022;50:W345-W351.
35. Mizuno H, Kitada K, Nakai K, Sarai A. PrognosScan: a new database for meta-analysis of the prognostic value of genes. *BMC Med Genomics*. 2009;2:18.
36. Goldman MJ, Craft B, Hastie M, et al. Visualizing and interpreting cancer genomics data via the Xena platform. *Nat Biotechnol*. 2020;38:675-678.
37. Staunton JE, Slonim DK, Collier HA, et al. Chemosensitivity prediction by transcriptional profiling. *Proc Natl Acad Sci U S A*. 2001;98:10787-10792.
38. Sanjana NE, Shalem O, Zhang F. Improved vectors and genome-wide libraries for CRISPR screening. *Nat Methods*. 2014;11:783-784.
39. Hart SN, Zhong XB. P450 oxidoreductase: genetic polymorphisms and implications for drug metabolism and toxicity. *Expert Opin Drug Metab Toxicol*. 2008;4:439-452.
40. Cahill MA, Jazayeri JA, Catalano SM, Toyokuni S, Kovacevic Z, Richardson DR. The emerging role of progesterone receptor membrane component 1 (PGRMC1) in cancer biology. *Biochim Biophys Acta*. 2016;1866:339-349.
41. Kabe Y, Nakane T, Koike I, et al. Haem-dependent dimerization of PGRMC1/Sigma-2 receptor facilitates cancer proliferation and chemoresistance. *Nat Commun*. 2016;7:11030.
42. Avvakumov N, Lalonde ME, Saksouk N, et al. Conserved molecular interactions within the HBO1 acetyltransferase complexes regulate cell proliferation. *Mol Cell Biol*. 2012;32:689-703.
43. Lalonde ME, Avvakumov N, Glass KC, et al. Exchange of associated factors directs a switch in HBO1 acetyltransferase histone tail specificity. *Genes Dev*. 2013;27:2009-2024.
44. Quintela M, Sieglaff DH, Gazze AS, et al. HBO1 directs histone H4 specific acetylation, potentiating mechano-transduction pathways and membrane elasticity in ovarian cancer cells. *Nanomedicine*. 2019;17:254-265.
45. Blackford AN, Jackson SP. ATM, ATR, and DNA-PK: the trinity at the heart of the DNA damage response. *Mol Cell*. 2017;66:801-817.
46. Saldívar JC, Cortez D, Cimprich KA. The essential kinase ATR: ensuring faithful duplication of a challenging genome. *Nat Rev Mol Cell Biol*. 2017;18:622-636.
47. Neizer-Ashun F, Bhattacharya R. Reality CHEK: understanding the biology and clinical potential of CHK1. *Cancer Lett*. 2021;497:202-211.
48. Podhorecka M, Skladanowski A, Bozko P. H2AX phosphorylation: its role in DNA damage response and cancer therapy. *J Nucleic Acids*. 2010;2010:920161.
49. Stope MB. Phosphorylation of histone H2A.X as a DNA-associated biomarker (review). *World Acad Sci J*. 2021;3:31.
50. Smela ME, Currier SS, Bailey EA, Essigmann JM. The chemistry and biology of aflatoxin B₁: from mutational spectrometry to carcinogenesis. *Carcinogenesis*. 2001;22:535-545.
51. Caldecott KW. Single-strand break repair and genetic disease. *Nat Rev Genet*. 2008;9:619-631.
52. Gohil D, Sarker AH, Roy R. Base excision repair: mechanisms and impact in biology, disease, and medicine. *Int J Mol Sci*. 2023;24:14186.
53. Yu X, Yustein JT, Xu J. Research models and mesenchymal/epithelial plasticity of osteosarcoma. *Cell Biosci*. 2021;11:94.
54. De Craene B, Gilbert B, Stove C, Bruyneel E, van Roy F, Bex G. The transcription factor snail induces tumor cell invasion through modulation of the epithelial cell differentiation program. *Cancer Res*. 2005;65:6237-6244.
55. Chen F, Chen C, Yang S, et al. Let-7b inhibits human cancer phenotype by targeting cytochrome P450 epoxygenase 2J2. *PLoS ONE*. 2012;7:e39197.
56. Saksouk N, Avvakumov N, Champagne KS, et al. HBO1 HAT complexes target chromatin throughout gene coding regions via

multiple PHD finger interactions with histone H3 tail. *Mol Cell*. 2009;33:257-265.

57. Hung T, Binda O, Champagne KS, et al. ING4 mediates crosstalk between histone H3 K4 trimethylation and H3 acetylation to attenuate cellular transformation. *Mol Cell*. 2009;33:248-256.
58. Lan R, Wang Q. Deciphering structure, function and mechanism of lysine acetyltransferase HBO1 in protein acetylation, transcription regulation, DNA replication and its oncogenic properties in cancer. *Cell Mol Life Sci*. 2020;77:637-649.
59. Li S, Hu J, Zhang L, et al. In-vitro and in-vivo evaluation of austocystin D liposomes. *J Pharm Pharmacol*. 2013;65:355-362.
60. Kong C, Yan X, Zhu Y, et al. *Fusobacterium nucleatum* promotes the development of colorectal cancer by activating a cytochrome P450/Epoxyoctadecenoic acid Axis via TLR4/Keap1/NRF2 signaling. *Cancer Res*. 2021;81:4485-4498.

SUPPORTING INFORMATION

Additional supporting information can be found online in the Supporting Information section at the end of this article.

How to cite this article: Kojima Y, Fujieda S, Zhou L, et al. Cytochrome P450 2J2 is required for the natural compound austocystin D to elicit cancer cell toxicity. *Cancer Sci*. 2024;115:3054-3066. doi:[10.1111/cas.16289](https://doi.org/10.1111/cas.16289)